

New ZrB₂ polymorphs: First-principles calculations

Marcin Maździarz*, Tomasz Mościcki

*Institute of Fundamental Technological Research Polish Academy of Sciences, Pawińskiego
5B, 02-106 Warsaw, Poland*

Abstract

Two new hypothetical zirconium diboride (ZrB₂) polymorphs: (*hP6*-P6₃/mmc-space group, no.194) and (*oP6*-Pmmn-space group, no.59), were thoroughly studied under the first-principles density functional theory calculations from the structural, mechanical and thermodynamic properties point of view. As opposed to the known phase (*hP3*-P6/mmm-space group, no.191) are not brittle. Knowledge about these new phases can be very useful when doping metal borides with zirconium.

Keywords: Zirconium diboride, *Ab initio* calculations, Mechanical properties, Elastic properties, Phonons

1. Introduction

During latest years the transition metal borides due to combination of their outstanding physical properties such as electric and thermal conductivity comparable with metals, low compressibility, high shear strength, and exceptionally high hardness have attracted attention among materials researchers [1, 2]. Even in the form of thin films they poses extraordinary properties such as very high hardness with increased flexibility, great thermal properties and very good corrosion and wear resistance [3, 4, 5]. Among borides, zirconium diboride (ZrB₂) deserves special attention. ZrB₂ with melting temperature 3245°C [6]

*Corresponding author

Email address: mmazdz@ipt.pan.pl (Marcin Maździarz)

is a member of a family of materials known as ultra high-temperature ceramics (UHTCs). In addition to high melting temperatures, ZrB_2 has a unique combination of chemical stability, high electrical and thermal conductivities, resistance to erosion and corrosion that makes it suitable for the extreme chemical and thermal environments associated with for example hypersonic flight, atmospheric re-entry, and rocket propulsion [7]. According to the ZrB phase diagram [8, 9] there are three phases, namely, ZrB, ZrB_2 , and ZrB_{12} , which have been reported and widely studied for this system. Theoretical investigations show that ZrB can create different crystallographic structures. The basic phase is NaCl-type face-centered cubic ZrB ($Fm\bar{3}m$ -space group, no.225) with lattice constant $a = 4.900\text{\AA}$ [10]. Furthermore, ZrB also can crystallize in FeB - type structure with a primitive orthorhombic (Pnma) crystal structure [9, 11], CrB-type orthorhombic structure with $Cmcm$ -space group [11, 12] and hexagonal $Pmmm$ [13]. The literature review shows, ZrB_{12} is stable in only one structure type. The cubic ZrB_{12} structure ($Fm\bar{3}m$ -space group, no.225) with lattice constant $a = 7.4085\text{\AA}$ was studied theoretically and experimentally for example in [14]. They compared electric-field gradient measurements at the B sites and first-principles calculations in order to analyse the chemical bonding properties. Both, experimental and theoretical results were in good agreement. Whereas in [15] the mechanical properties of ZrB_{12} were calculated. The Vickers hardness of zirconium boride was 32.9 GPa, which is in good agreement with the other theoretical result [14, 16, 17].

In contrast to ZrB_{12} , depending on the calculation method, different hardness values have been determined for zirconium diboride ZrB_2 . The calculated [18] values of hardness range from 12.82 GPa to 55.53 GPa, whereas experimentally measured hardness reaches 23 ± 0.9 GPa [6, 19]. All mentioned structures were assigned as ZrB_2 with the crystal hexagonal structure of AlB_2 -type with the $P6/mmm$ -space group, no.191. Such large differences in the values of the analysed properties may, however, come not only from differences in calculation methods but also from the possibility of existence of other stable forms of ZrB_2 which may form nanocomposite of different polymorphs of ZrB_2 . A

similar conclusion about the possibility of existence of other ZrB_2 crystal types can be drawn on the basis of other studies on possible forms of transition metal diborides, e.g. WB_2 [20, 21] or ReB_2 [22, 23]. For comparison in [21] the Authors proposed six different phases of WB_2 . In the case of ZrB_2 is hard to find such study.

It should be also noted that in addition to the phases appearing in the Zr-B equilibrium diagram [8, 24], other zirconium and boron compounds were theoretically determined. There are hypothetical Zr-B phases such as: Zr_3B_4 , Zr_2B_3 , Zr_3B_2 [16], ZrB_3 [25], ZrB_4 [26] and ZrB_6 [13]. All polymorphs are both mechanically and dynamically stable but have not been confirmed experimentally yet. In this work structural, mechanical and thermodynamic properties of stable ZrB_2 polymorphs from density functional calculations will be studied.

2. Computational methods

First-principle calculations based on density functional theory (DFT) [27, 28] within the pseudopotential, plane-wave approximation (PP-PW) implemented in ABINIT [29, 30] code were performed in this work. Projector augmented-wave formulation (PAW) pseudopotentials [31] were used to describe the interactions of ionic core and non-valence electrons.

To enhance the confidence of the calculations as an exchange-correlation (XC) functional three approximations were used: local density approximation (LDA) [32, 33], classical Perdew-Burke-Ernzerhof (PBE) generalized gradient approximation (GGA) [34] and modified Perdew-Burke-Ernzerhof GGA for solids (PBEsol) [35]. There is a strong view that the PBEsol is the overall best performing XC functional for identifying the structure and elastic properties [36, 37, 38].

Used PAW pseudopotentials for LDA and PBE XC functionals were taken from PseudoDojo project [39]. Projector augmented wave method (PAW) pseudopotentials for PBEsol exchange-correlation functional [35] were generated using ATOMPAW software [40] and a library of exchange-correlation functionals

for density functional theory LibXC [41].

All calculations were made by tuning the precision of the calculations by automatically setting the variables at *accuracy* level 4. The *cut-off* energy consistent with (PAW) pseudopotentials of the plane-wave basis set was 15 Ha with the $4d^25s^2$ valence electrons for Zr and $2s^22p^1$ valence electrons for B. K-PoinTs grid was generated with *kptrlen*=30.0. Metallic occupation of levels with Fermi-Dirac smearing occupation scheme and *tsmear* (Ha) = 0.02 was used in all ABINIT calculations.

2.1. Optimization of structures

As mentioned earlier tungsten diboride [20] and rhenium diboride [23] crystallize in many various space groups. Searching for new structures of ZrB_2 we started with basic cells of *hP6*- $P6_3/mmc$ - WB_2 and *oP6*- $Pmmn$ - WB_2 and replaced tungsten atoms by zirconium atoms. Then all structures were relaxed by using the Broyden-Fletcher-Goldfarb-Shanno minimization scheme (BFGS) with full optimization of cell geometry and atomic coordinates. Maximal stress tolerance (GPa) was set to 1×10^{-4} .

2.2. Formation enthalpy and Cohesive energy

The formation enthalpy and cohesive energy were determined as follows [42, 23]:

$$\Delta_f H(ZrB_2) = E_{coh}(ZrB_2) - E_{coh}(Zr) - 2E_{coh}(B), \quad (1)$$

$$E_{coh}(ZrB_2) = E_{total}(ZrB_2) - E_{iso}(Zr) - 2E_{iso}(B), \quad (2)$$

where $\Delta_f H(ZrB_2)$ is the formation enthalpy of the ZrB_2 ; $E_{coh}(ZrB_2)$ is the cohesive energy of the ZrB_2 ; $E_{coh}(Zr)$ is the cohesive energy of Zr ; $E_{coh}(B)$ is the cohesive energy of B ; $E_{tot}(ZrB_2)$ is the total energy of the ZrB_2 ; $E_{iso}(Zr)$ is the total energy of a Zr atom and $E_{iso}(B)$ is the total energy of a B atom.

2.3. Mechanical properties calculations

The theoretical ground state elastic constants C_{ij} of all structures were established with the metric tensor formulation of strain in density functional perturbation theory (DFPT) [43]. Isotropised bulk modulus B , shear modulus G , Young's modulus E and Poisson's ratio ν were estimated by means of a *VoigtReussHill* average [44, 45].

In order to verify the elastic stability of all the structures positive definiteness of the stiffness tensor was checked [46] by calculating Kelvin moduli, i.e. eigenvalues of stiffness tensor represented in *second-rank tensor* notation [47].

Hardness of ZrB₂ polymorphs in the present paper was calculated with the use of semi-empirical relation proposed in [48]. The equation is defined as follow:

$$H_v = 0.92(G/B)^{1.137}G^{0.708}. \quad (3)$$

G/B ratio appearing in the above formula named Pugh's modulus ratio [49] is commonly used as a universal ductile-to-brittle criterion.

2.4. Phonon and Thermodynamic properties calculations

To calculate phonons, density functional perturbation theory (DFPT) was utilised [29, 30]. The phonon dispersion curves [50] of the analysed structures were then used to determine their dynamical stability [46, 51] complementary to elastic stability. Acoustic Debye temperature was calculated from the phonon densities of states (DOS).

Using the calculated phonons under the harmonic approximation, i.e. in the range up to Debye temperature, thermal quantities: phonon internal energy, free energy, entropy, constant volume heat capacity as a function of the temperature were determined [24, 52].

3. Results

Using the approach described in Sec.2.1 the first step in our calculations was the geometry optimization of the two new hypothetical zirconium diboride

(ZrB₂) polymorphs: (*hP6*-P6₃/mmc-space group, no.194) and (*oP6*-Pmmn-space group, no.59) and the formerly known polymorph (*hP3*-P6/mmm-space group, no.191).

3.1. Structural properties

The basic cells for all three analysed polymorphs are depicted in Fig.1, whereas the crystallographic data, calculated with three different exchange-correlation (XC) functionals (LDA, PBE and PBEsol), are stored in Crystallographic Information Files (CIF) in Appendix A. Supplementary data.

Determined lattice parameters, formation enthalpy and cohesive energy for known *hP3*-P6/mmm polymorph, Fig.1 a), are comparable to those of other authors [18], see Tab.1. We treat this as a verification of the correctness of the methodology used.

The first new hypothetical phase *hP6*-P6₃/mmc, Fig.1 b), also crystallises in the hexagonal system but has 6 atoms in the cell, whereas the second new hypothetical phase *oP6*-Pmmn, Fig.1 c), crystallises in the orthorhombic system and also has 6 atoms in the cell. There is a little sense to compare lattice parameters for phases in different systems, but it is worth to compare the formation enthalpy and the cohesive energy. It can be seen that the formation enthalpy $\Delta_f H$ for new phases is significantly higher than for known *hP3*-P6/mmm and comparable between the new phases, see Tab.1. The calculated cohesive energy E_c is a little higher than for known *hP3*-P6/mmm and again comparable between the two new phases. These two facts suggest that the new phases are comparably thermodynamically stable but less stable than the known *hP3*-P6/mmm phase.

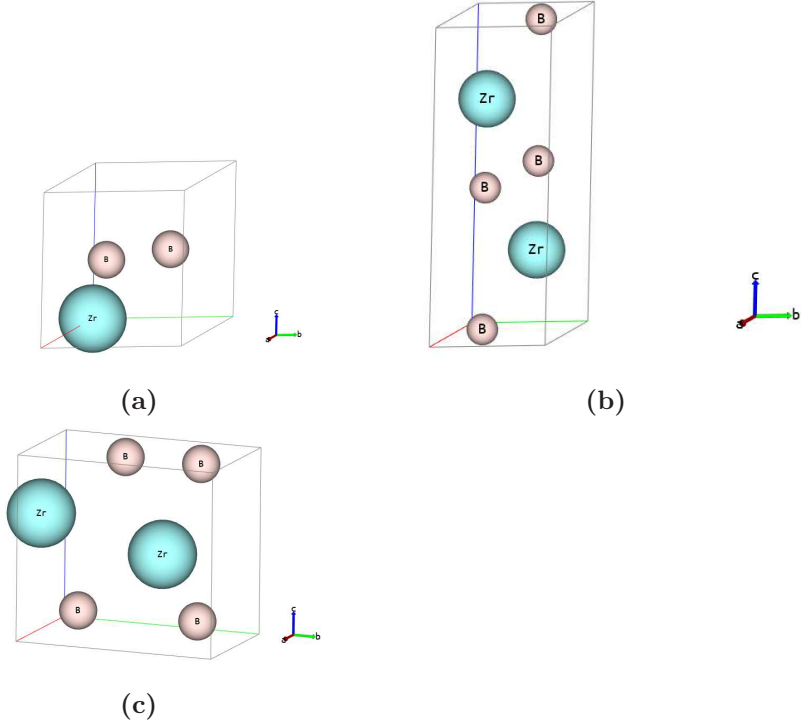


Figure 1: ZB₂-Basic cells: a) $hP3$ -P6/mmm, b) $hP6$ -P6₃/mmc, c) $oP6$ -Pmnn

3.2. Mechanical properties

Computed elastic constants, Kelvin moduli, isotropised bulk, shear and Young's modulus, Poisson's ratio, G/B Pugh's modulus ratio, Debye temperature and estimated hardness of all analysed zirconium diboride structures are listed in Tab.1. For known $hP3$ -P6/mmm phase, Fig.1 a), these quantities are comparable to those of other authors [18], what is a further verification of the validity of the methodology used. Analysing the data received, it can be concluded that the new phases have lower mechanical parameters than the known $hP3$ -P6/mmm phase, except for the Poisson's ratio. Both new phases have similar isotropised bulk modulus of about 170 GPa, but the shear modulus for the $hP6$ -P6₃/mmc phase is much lower and is only about 40 GPa. The consequence of this is that the hardness for $hP6$ -P6₃/mmc phase is only 2 GPa, while for

oP6-Pmmn phase it is about 14 GPa. A high G/B Pugh's modulus ratio would correspond to a more brittle character of material than ductile. The critical value, separating ductile from brittle materials, is approximately 0.571 [49, 53]. It can be seen that known *hP3*-P6/mmm phase is brittle, *hP6*-P6₃/mmc phase is ductile and *oP6*-Pmmn phase is somehow between brittle and ductile.

All analysed structures have positive definite stiffness tensor, positive Kelvin moduli, i.e. eigenvalues of stiffness tensor represented in *second-rank tensor* notation, so there are mechanically stable, see Tab.1.

Table 1: Lattice parameters (\AA), formation enthalpy $\Delta_f H$ (eV/Atom), cohesive energy E_c (eV/Atom), elastic constants C_{ij} (GPa), Kelvin moduli K_i (GPa), bulk modulus B (GPa), shear modulus G (GPa), Young's modulus E (GPa), Poisson's ratio ν , G/B Pugh's modulus ratio, Debye temperature Θ_D (K), hardness H_v (GPa) of ZrB_2 phases: $\text{ZrB}_2(hP3\text{-}P6/\text{mmm}$ -space group, no.191, $hP6\text{-}P6_3/\text{mmc}$ -space group, no.194, $oP6\text{-}P6/\text{mmm}$ -space group, no.59). Experimental and calculated data for $hP3\text{-}P6/\text{mmm}$ phase are taken from [18].

Phase	$hP3\text{-}P6/\text{mmm}$ -No.191			$hP6\text{-}P6_3/\text{mmc}$ -No.194			$oP6\text{-}P6/\text{mmm}$ -No.59				
	Source	Exp./Calc.	LDA	PBE	PBEsol	LDA	PBE	PBEsol	LDA	PBE	PBEsol
a		3.165÷3.169	3.135	3.173	3.156	3.025	3.076	3.050	3.057	3.100	3.071
b									4.931	5.029	4.981
c		3.523÷3.547	3.477	3.527	3.495	8.515	8.624	8.565	4.541	4.604	4.578
$-\Delta_f H$		0.985÷1.099	1.145	1.078	1.141	4.023	3.691	3.853	3.795	3.654	3.813
$-E_c$		8.648	8.769	8.072	8.411	7.834	7.187	7.488	7.187	7.150	7.448
C_{11}		581	618	591	597	224	214	217	333	325	336
C_{22}		581	618	591	597	224	214	217	331	316	334
C_{33}		445	477	481	456	495	447	479	436	380	439
C_{44}		240	278	253	269	81	73	80	136	134	144
C_{55}		240	278	253	269	81	73	80	43	48	35
C_{66}		263	283	272	274	1	9	2	122	145	126
C_{12}		55	52	47	49	222	196	213	111	80	109
C_{13}		121	135	105	126	70	63	69	97	70	88
C_{23}		121	135	105	126	70	63	69	99	85	92
K_I			787	727	753	572	519	555	578	500	569
K_{II}			566	544	548	162	146	160	301	290	314
K_{III}			566	544	548	162	146	160	272	283	288
K_{IV}			556	506	538	2	18	4	244	268	252
K_V			556	506	538	2	18	4	221	238	226
K_{VI}			360	392	349	369	338	354	86	96	70
B		220÷245	262	242	250	184	168	178	189	165	187
G		225÷243	256	247	248	37	44	37	102	108	100
E		502÷554	580	554	560	104	121	105	260	267	256
ν		0.109÷0.13	0.13	0.118	0.126	0.406	0.38	0.402	0.271	0.231	0.272
G/B		1.023÷0.992	0.981	1.024	0.995	0.200	0.261	0.21	0.541	0.655	0.539
Θ_D		910	1007	973	971	794	754	779	787	752	774
H_v		23÷55	46	47	45	2	3	2	12	16	12

3.3. Phonon and Thermodynamic properties

Phonon dispersion curves along the high symmetry q-points [50] and phonon densities of states (DOS) calculated with the use of PBEsol exchange-correlation

(XC) functional for known $hP3$ -P6/mmm phase, Fig.1 a), are depicted in Fig.2, for the phase $hP6$ -P6₃/mmc, Fig.1 b), in Fig.3 and for the phase $oP6$ -Pmmn, Fig.1 c), in Fig.4, respectively. Phonon results for all exchange-correlation (XC) functionals are stored in Appendix A. Supplementary data. Analysis of the calculated curves allows us to state that phonon modes everywhere have positive frequencies and the new ZrB₂ phases are not only mechanically but also dynamically stable. The estimated acoustic Debye temperature Θ_D for the two new proposed ZrB₂ phases is about 760 K and is about 200 K lower than that for the known $hP3$ -P6/mmm phase and it is consistent with the mechanical properties, see Tab.1. Results for thermodynamic properties up to 760 K for the three zirconium diboride polymorphs calculated with the use of PBEsol exchange-correlation (XC) functional, i.e. phonon internal energy, free energy, entropy, constant volume heat capacity are depicted in Figs.5, 6, 7 and it can be seen that are very similar for the two new proposed ZrB₂ polymorphs. This additional fact suggests again that the new phases are comparably thermodynamically stable up to Debye temperature Θ_D , but less stable than the known $hP3$ -P6/mmm phase.

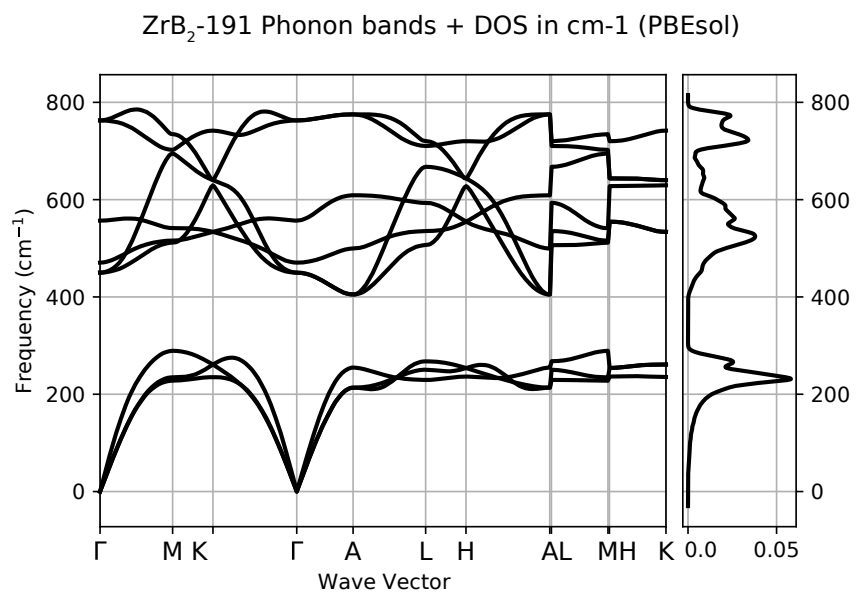


Figure 2: ZrB₂(*hP3*-P6/*mmm*-space group, no.191)-Phonon band structure and DOS.

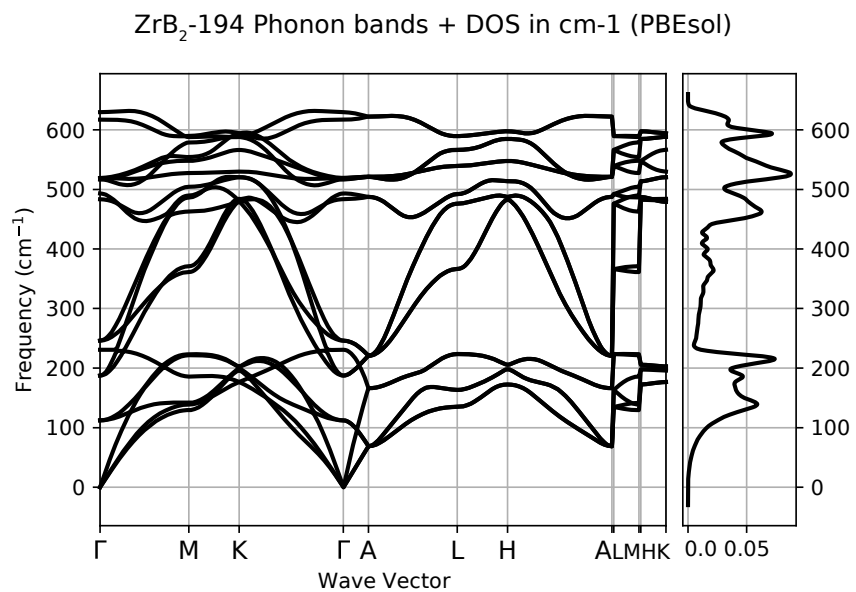


Figure 3: ZrB₂(*hP6*-P6₃/*mmc*-space group, no.194)-Phonon band structure and DOS.

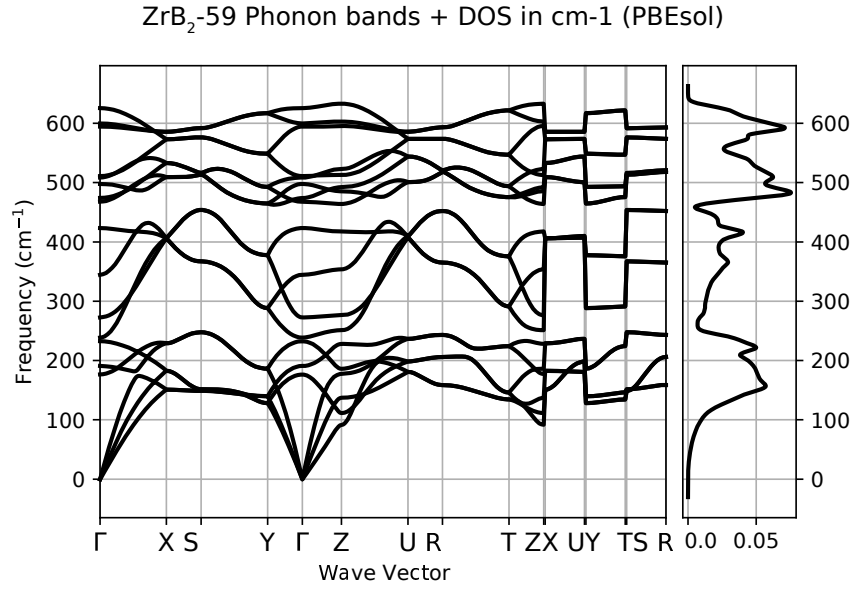


Figure 4: ZrB₂(*oP6*-P6/*mmm*-space group, no.59)-Phonon band structure and DOS.

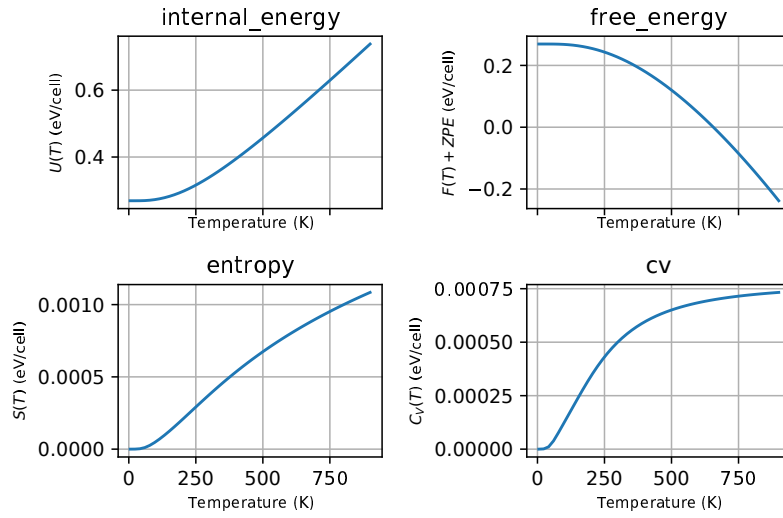


Figure 5: ZrB₂(*hP3*-P6/*mmm*-space group, no.191)-Thermodynamic properties: internal energy, free energy, entropy and constant-volume specific heat.

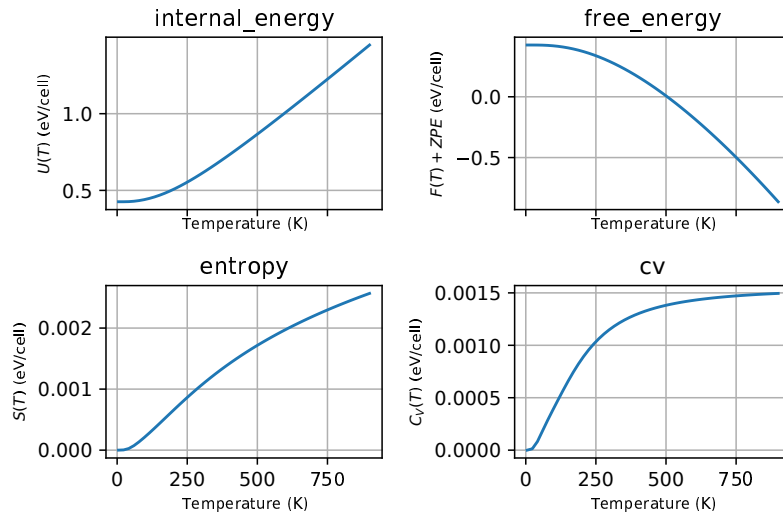


Figure 6: ZrB_2 (*hP6*-*P6*₃/*mmc*-space group, no.194)-Thermodynamic properties: internal energy, free energy, entropy and constant-volume specific heat.

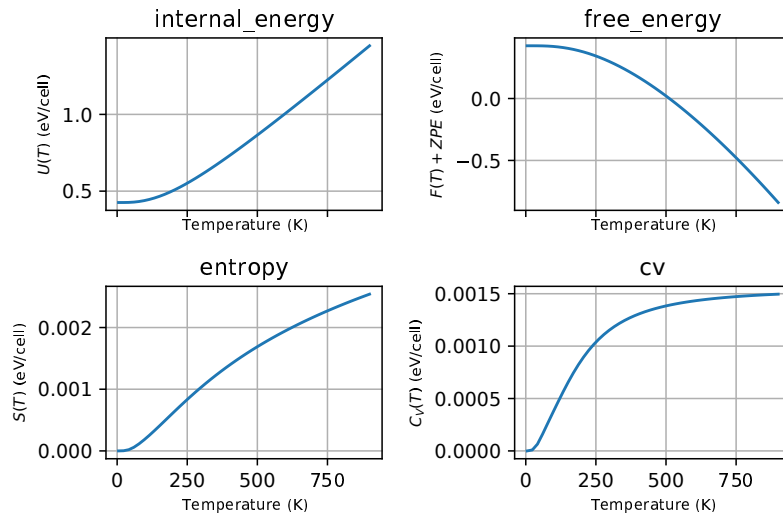


Figure 7: ZrB_2 (*oP6*-*P6*/*mmm*-space group, no.59)-Thermodynamic properties: internal energy, free energy, entropy and constant-volume specific heat.

4. Conclusions

In the present paper extensive analysis of two new hypothetical and one previously known zirconium diboride (ZrB_2) polymorphs within the framework of density functional theory from the structural, mechanical and thermodynamic properties point of view was performed. We can conclude that:

- two new hypothetical zirconium diboride (ZrB_2) polymorphs: ($hP6$ - $P6_3/mmc$ -space group, no.194) and ($oP6$ - $Pmmm$ -space group, no.59) are mechanically and dynamically stable,
- these phases are comparably thermodynamically stable but less stable than the known $hP3$ - $P6/mmm$ phase,
- $hP6$ - $P6_3/mmc$ phase is ductile and $oP6$ - $Pmmm$ phase is intermediate between brittle and ductile,
- both new phases have a lower hardness than the known $hP3$ - $P6/mmm$ phase.

Many results in the paper, particularly relating to new hypothetical zirconium diboride (ZrB_2) polymorphs, are the first to be notified and we trust will be confirmed by other studies.

ACKNOWLEDGMENTS

This work was supported by the National Science Centre (NCN – Poland) Research Project: UMO-2017/25/B/ST8/01789. Additional assistance was granted through the computing cluster GRAFEN at Biocentrum Ochota, the Interdisciplinary Centre for Mathematical and Computational Modelling of Warsaw University (ICM UW) and Poznań Supercomputing and Networking Center (PSNC).

Appendix A. Supplementary data

Supplementary data to this article can be found online at Supplementary Information.

References

- [1] G. Akopov, M. T. Yeung, R. B. Kaner, Rediscovering the Crystal Chemistry of Borides, *Advanced Materials* 29 (21) (2017) 1604506. doi:10.1002/adma.201604506.
- [2] G. Akopov, L. E. Pangilinan, R. Mohammadi, R. B. Kaner, Perspective: Superhard metal borides: A look forward, *APL Materials* 6 (7) (2018) 070901. doi:10.1063/1.5040763.
- [3] C. Fuger, V. Moraes, R. Hahn, H. Bolvardi, P. Polcik, H. Riedl, P. H. Mayrhofer, Influence of Tantalum on phase stability and mechanical properties of WB_2 , *MRS Communications* 9 (1) (2019) 375380. doi:10.1557/mrc.2019.5.
- [4] S. Mirzaei, M. Alishahi, P. Souek, J. enek, D. Holec, N. Koutn, V. Burkov, M. Stupavsk, L. Zbransk, F. Burmeister, B. Blug, Z. Czigny, K. Balzsi, R. Mikov, P. Vaina, The effect of chemical composition on the structure, chemistry and mechanical properties of magnetron sputtered W-B-C coatings: Modeling and experiments, *Surface and Coatings Technology* 383 (2020) 125274. doi:10.1016/j.surfcoat.2019.125274.
- [5] T. Moscicki, R. Psiuk, H. Somiska, N. Levintant-Zayonts, D. Garbiec, M. Pisarek, P. Bazarnik, S. Nosewicz, J. Chrzanowska-Giyska, Influence of overstoichiometric boron and titanium addition on the properties of rf magnetron sputtered tungsten borides, *Surface and Coatings Technology* 390 (2020) 125689. doi:10.1016/j.surfcoat.2020.125689.
- [6] W. G. Fahrenholtz, G. E. Hilmas, I. G. Talmy, J. A. Zaykoski, Refractory Diborides of Zirconium and Hafnium, *Journal of the American Ceramic Society* 90 (5) (2007) 1347–1364. doi:10.1111/j.1551-2916.2007.01583.x.
- [7] M. M. Opeka, I. G. Talmy, J. A. Zaykoski, Oxidation-based materials selection for 2000C + hypersonic aerosurfaces: Theoretical considerations and

- historical experience, *Journal of Materials Science* 39 (2004) 5887–5904.
doi:10.1023/B:JMSC.0000041686.21788.77.
- [8] H. Chen, F. Zheng, H. Liu, L. Liu, Z. Jin, Thermodynamic assessment of BZr and SiZr binary systems, *Journal of Alloys and Compounds* 468 (1) (2009) 209 – 216. doi:10.1016/j.jallcom.2008.01.061.
- [9] T. Tokunaga, K. Terashima, H. Ohtani, M. Hasebe, Thermodynamic Analysis of the Phase Equilibria in the Fe-Zr-B System, *MATERIALS TRANSACTIONS* 49 (11) (2008) 2534–2540. doi:10.2320/matertrans.MB200809.
- [10] H. Li, L. Zhang, Q. Zeng, J. Wang, L. Cheng, H. Ren, K. Guan, Crystal structure and elastic properties of ZrB compared with ZrB₂: A first-principles study, *Computational Materials Science* 49 (4) (2010) 814 – 819. doi:10.1016/j.commatsci.2010.06.027.
- [11] B. Huang, Y.-H. Duan, W.-C. Hu, Y. Sun, S. Chen, Structural, anisotropic elastic and thermal properties of MB (M=Ti, Zr and Hf) monoborides, *Ceramics International* 41 (5, Part B) (2015) 6831 – 6843. doi:10.1016/j.ceramint.2015.01.132.
- [12] X. Xu, K. Fu, L. Li, Z. Lu, X. Zhang, Y. Fan, J. Lin, G. Liu, H. Luo, C. Tang, Dependence of the elastic properties of the early-transition-metal monoborides on their electronic structures: A density functional theory study, *Physica B: Condensed Matter* 419 (2013) 105 – 111. doi:10.1016/j.physb.2013.03.018.
- [13] X. Li, F. Peng, Predicted superhard phases of ZrB compounds under pressure, *Phys. Chem. Chem. Phys.* 21 (2019) 15609–15614. doi:10.1039/C9CP01775E.
- [14] B. Jger, S. Paluch, O. J. Żogał, W. Wolf, P. Herzig, V. B. Filippov, N. Shitsevalova, Y. Paderno, Characterization of the electronic properties of YB₁₂, ZrB₁₂, and LuB₁₂ using ¹¹B NMR and first-principles cal-

- culations, *Journal of Physics: Condensed Matter* 18 (8) (2006) 2525–2535. doi:10.1088/0953-8984/18/8/015.
- [15] Y. Pan, Y. Lin, Influence of alloying elements on the mechanical and thermodynamic properties of ZrB_{12} ceramics from first-principles calculations, *International Journal of Quantum Chemistry* 120 (12) (2020) e26217. doi:10.1002/qua.26217.
- [16] J. Li, C. Fan, Novel metastable compounds in the ZrB system: an ab initio evolutionary study, *Phys. Chem. Chem. Phys.* 17 (2015) 1180–1188. doi:10.1039/C4CP04185B.
- [17] Z.-Q. Chen, Y.-S. Peng, M. Hu, C.-M. Li, Y.-T. Luo, Elasticity, hardness, and thermal properties of ZrB_n ($n=1, 2, 12$), *Ceramics International* 42 (6) (2016) 6624 – 6631. doi:10.1016/j.ceramint.2015.12.175.
- [18] X. Zhang, X. Luo, J. Han, J. Li, W. Han, Electronic structure, elasticity and hardness of diborides of zirconium and hafnium: First principles calculations, *Computational Materials Science* 44 (2) (2008) 411 – 421. doi:10.1016/j.commatsci.2008.04.002.
- [19] A. Chamberlain, W. Fahrenholtz, G. Hilmas, D. Ellerby, HighStrength Zirconium DiborideBased Ceramics, *Journal of the American Ceramic Society* 87 (2008) 1170 – 1172. doi:10.1111/j.1551-2916.2004.01170.x.
- [20] M. Maździarz, T. Mościcki, Structural, mechanical and optical properties of potentially superhard WB_x polymorphs from first principles calculations, *Materials Chemistry and Physics* 179 (2016) 92 – 102. doi:10.1016/j.matchemphys.2016.05.014.
- [21] X.-Y. Cheng, X.-Q. Chen, D.-Z. Li, Y.-Y. Li, Computational materials discovery: the case of the W–B system, *Acta Crystallographica Section C* 70 (2) (2014) 85–103. doi:10.1107/S2053229613027551.
- [22] M. Marn-Surez, M. Velez, J. David, M. Arroyave, Mechanical properties study for new hypothetical crystalline phases of ReB_2 : A computational

- approach using density functional theory, *Computational Materials Science* 122 (2016) 240–248. doi:10.1016/j.commatsci.2016.05.032.
- [23] M. Maździarz, T. Mościcki, Structural, Mechanical, Optical, Thermodynamical and Phonon Properties of stable ReB₂ polymorphs from Density Functional calculations, *Journal of Alloys and Compounds* 657 (2016) 878 – 888. doi:10.1016/j.jallcom.2015.10.133.
- [24] A. Togo, I. Tanaka, First principles phonon calculations in materials science, *Scripta Materialia* 108 (2015) 1 – 5. doi:10.1016/j.scriptamat.2015.07.021.
- [25] G. Zhang, T. Bai, Y. Zhao, Y. Hu, A New Superhard Phase and Physical Properties of ZrB₃ from First-Principles Calculations, *Materials* 9 (8) (2016). doi:10.3390/ma9080703.
- [26] X. Zhang, J. Qin, X. Sun, Y. Xue, M. Ma, R. Liu, First-principles structural design of superhard material of ZrB₄, *Phys. Chem. Chem. Phys.* 15 (2013) 20894–20899. doi:10.1039/C3CP53893A.
- [27] P. Hohenberg, W. Kohn, Inhomogeneous electron gas, *Phys. Rev.* 136 (1964) B864–B871. doi:10.1103/PhysRev.136.B864.
- [28] W. Kohn, L. J. Sham, Self-consistent equations including exchange and correlation effects, *Phys. Rev.* 140 (1965) A1133–A1138. doi:10.1103/PhysRev.140.A1133.
- [29] X. Gonze, F. Jollet, F. A. Araujo, D. Adams, B. Amadon, T. Applencourt, C. Audouze, J.-M. Beuken, J. Bieder, A. Bokhanchuk, E. Bousquet, F. Bruneval, D. Caliste, M. Ct, F. Dahm, F. D. Pieve, M. Delaveau, M. D. Gennaro, B. Dorado, C. Espejo, G. Geneste, L. Genovese, A. Gerossier, M. Giantomassi, Y. Gillet, D. Hamann, L. He, G. Jomard, J. L. Janssen, S. L. Roux, A. Levitt, A. Lherbier, F. Liu, I. Lukaevi, A. Martin, C. Martins, M. Oliveira, S. Ponc, Y. Pouillon, T. Rangel, G.-M. Rignanese,

- A. Romero, B. Rousseau, O. Rubel, A. Shukri, M. Stankovski, M. Torrent, M. V. Setten, B. V. Troeye, M. Verstraete, D. Waroquiers, J. Wiktor, B. Xu, A. Zhou, J. Zwanziger, Recent developments in the ABINIT software package, *Computer Physics Communications* 205 (2016) 106 – 131. doi:10.1016/j.cpc.2016.04.003.
- [30] X. Gonze, B. Amadon, G. Antonius, F. Arnardi, L. Baguet, J.-M. Beuken, J. Bieder, F. Bottin, J. Bouchet, E. Bousquet, N. Brouwer, F. Bruneval, G. Brunin, T. Cavignac, J.-B. Charraud, W. Chen, M. Ct, S. Cottenier, J. Denier, G. Geneste, P. Ghosez, M. Giantomassi, Y. Gillet, O. Gingras, D. R. Hamann, G. Hautier, X. He, N. Helbig, N. Holzwarth, Y. Jia, F. Jollet, W. Lafargue-Dit-Hauret, K. Lejaeghere, M. A. Marques, A. Martin, C. Martins, H. P. Miranda, F. Naccarato, K. Persson, G. Petretto, V. Planes, Y. Pouillon, S. Prokhorenko, F. Ricci, G.-M. Rignanese, A. H. Romero, M. M. Schmitt, M. Torrent, M. J. van Setten, B. V. Troeye, M. J. Verstraete, G. Zrah, J. W. Zwanziger, The ABINIT project: Impact, environment and recent developments, *Computer Physics Communications* 248 (2020) 107042. doi:10.1016/j.cpc.2019.107042.
- [31] A. Martin, M. Torrent, R. Caracas, Projector augmented-wave formulation of response to strain and electric-field perturbation within density functional perturbation theory, *Phys. Rev. B* 99 (2019) 094112. doi:10.1103/PhysRevB.99.094112.
- [32] F. Bloch, Bemerkung zur Elektronentheorie des Ferromagnetismus und der elektrischen Leitfähigkeit, *Zeitschrift für Physik* 57 (1929) 545–555. doi:10.1007/BF01340281.
- [33] J. P. Perdew, Y. Wang, Accurate and simple analytic representation of the electron-gas correlation energy, *Phys. Rev. B* 45 (1992) 13244–13249. doi:10.1103/PhysRevB.45.13244.
- [34] J. P. Perdew, K. Burke, M. Ernzerhof, Generalized Gradient Ap-

- proximation Made Simple, *Phys. Rev. Lett.* 77 (1996) 3865–3868.
doi:10.1103/PhysRevLett.77.3865.
- [35] J. P. Perdew, A. Ruzsinszky, G. I. Csonka, O. A. Vydrov, G. E. Scuseria, L. A. Constantin, X. Zhou, K. Burke, Restoring the Density-Gradient Expansion for Exchange in Solids and Surfaces, *Phys. Rev. Lett.* 100 (2008) 136406. doi:10.1103/PhysRevLett.100.136406.
- [36] M. Råsander, M. A. Moram, On the accuracy of commonly used density functional approximations in determining the elastic constants of insulators and semiconductors, *The Journal of Chemical Physics* 143 (14) (2015) –. doi:10.1063/1.4932334.
- [37] M. Maździarz, A. Mrozek, W. Kuś, T. Burczyński, First-principles study of new X-graphene and Y-graphene polymorphs generated by the two stage strategy, *Materials Chemistry and Physics* 202 (2017) 7 – 14. doi:10.1016/j.matchemphys.2017.08.066.
- [38] M. Maździarz, A. Mrozek, W. Kuś, T. Burczyński, Anisotropic-Cyclicgraphene: A New Two-Dimensional Semiconducting Carbon Allotrope, *Materials* 11 (3) (2018) 432. doi:10.3390/ma11030432.
- [39] F. Jollet, M. Torrent, N. Holzwarth, Generation of Projector Augmented-Wave atomic data: A 71 element validated table in the XML format, *Computer Physics Communications* 185 (4) (2014) 1246 – 1254. doi:10.1016/j.cpc.2013.12.023.
- [40] N. Holzwarth, A. Tackett, G. Matthews, A Projector Augmented Wave (PAW) code for electronic structure calculations, Part I: atompaw for generating atom-centered functions, *Computer Physics Communications* 135 (3) (2001) 329 – 347. doi:10.1016/S0010-4655(00)00244-7.
- [41] S. Lehtola, C. Steigemann, M. J. Oliveira, M. A. Marques, Recent developments in LIBXC A comprehensive library of func-

- tionals for density functional theory, *SoftwareX* 7 (2018) 1 – 5. doi:10.1016/j.softx.2017.11.002.
- [42] C. Qi, Y. Jiang, Y. Liu, R. Zhou, Elastic and electronic properties of XB_2 ($\text{X}=\text{V}$, Nb , Ta , Cr , Mo , and W) with AlB_2 structure from first principles calculations, *Ceramics International* 40 (4) (2014) 5843 – 5851. doi:10.1016/j.ceramint.2013.11.026.
- [43] D. R. Hamann, X. Wu, K. M. Rabe, D. Vanderbilt, Metric tensor formulation of strain in density-functional perturbation theory, *Phys. Rev. B* 71 (2005) 035117. doi:10.1103/PhysRevB.71.035117.
- [44] R. Hill, The Elastic Behaviour of a Crystalline Aggregate, *Proceedings of the Physical Society. Section A* 65 (5) (1952) 349–354. doi:10.1088/0370-1298/65/5/307.
- [45] M. Maździarz, M. Gajewski, Estimation of Isotropic Hyperelasticity Constitutive Models to Approximate the Atomistic Simulation Data for Aluminium and Tungsten Monocrystals, *Computer Modeling in Engineering & Sciences* 105 (2) (2015) 123–150. doi:10.3970/cmes.2015.105.123.
- [46] G. Grimvall, B. Magyari-Köpe, V. Ozoliņš, K. A. Persson, Lattice instabilities in metallic elements, *Rev. Mod. Phys.* 84 (2012) 945–986. doi:10.1103/RevModPhys.84.945.
- [47] M. Maździarz, Comment on ‘The Computational 2D Materials Database: high-throughput modeling and discovery of atomically thin crystals’, *2D Materials* 6 (4) (2019) 048001. doi:10.1088/2053-1583/ab2ef3.
- [48] Y. Tian, B. Xu, Z. Zhao, Microscopic theory of hardness and design of novel superhard crystals, *International Journal of Refractory Metals and Hard Materials* 33 (0) (2012) 93 – 106. doi:10.1016/j.ijrmhm.2012.02.021.
- [49] S. Pugh, XCII. Relations between the elastic moduli and the plastic properties of polycrystalline pure metals, *The London, Edinburgh, and Dublin*

Philosophical Magazine and Journal of Science 45 (367) (1954) 823–843.
doi:10.1080/14786440808520496.

- [50] Y. Hinuma, G. Pizzi, Y. Kumagai, F. Oba, I. Tanaka, Band structure diagram paths based on crystallography, *Computational Materials Science* 128 (2017) 140 – 184. doi:10.1016/j.commatsci.2016.10.015.
- [51] P. Řehák, M. Černý, J. Pokluda, Dynamic stability of fcc crystals under isotropic loading from first principles, *Journal of Physics: Condensed Matter* 24 (21) (2012) 215403. doi:10.1088/0953-8984/24/21/215403.
- [52] F. Bottin, J. Bieder, J. Bouchet, A-TDEP: Temperature Dependent Effective Potential for ABINIT Lattice dynamic properties including anharmonicity, *Computer Physics Communications* (2020) 107301doi:10.1016/j.cpc.2020.107301.
- [53] H. Rached, D. Rached, S. Benalia, A. Reshak, M. Rabah, R. Khenata, S. B. Omran, First-principles study of structural stabilities, elastic and electronic properties of transition metal monocarbides (TMCs) and mononitrides (TMNs) , *Materials Chemistry and Physics* 143 (1) (2013) 93 – 108. doi:10.1016/j.matchemphys.2013.08.020.